

Bayesian model selection approach for colored graphical Gaussian models

Qiong Li ^a Xin Gao ^{*} H el ene Massam [†]

^a School of Mathematics (Zhuhai), Sun Yat-sen University, Zhuhai, 519082, Guangdong, China

^{*} [†] Department of Mathematics and Statistics, York University, Toronto, M3J1P3, Canada

April 3, 2020

Abstract

We consider a class of colored graphical Gaussian models obtained by placing symmetry constraints on the precision matrix in a Bayesian framework. The prior distribution on the precision matrix is the colored G -Wishart prior which is the Diaconis-Ylvisaker conjugate prior. In this paper, we develop a computationally efficient model search algorithm which combines linear regression with a double reversible jump Markov chain Monte Carlo (MCMC) method. The latter is to estimate the Bayes factors expressed as the ratio of posterior probabilities of two competing models. We also establish the asymptotic consistency property of the model selection procedure based on the Bayes factors. Our procedure avoids an exhaustive search which is computationally impossible. Our method is illustrated with simulations and a real-world application with a protein signalling data set.

Keywords: Auxiliary variable MCMC algorithm; Colored G -Wishart distribution; Double reversible jump

^{*}To whom correspondence should be addressed. Email: xingao@mathstat.yorku.ca

[†]^{*}Supported in part by the Natural Sciences and Engineering Research Council of Canada (NSERC) individual discovery grants.

1 Introduction

Graphical models provide an effective way to determine conditional independence relationships in high-dimensional data. Application of these models arise in the study of gene expression data (Dobra et al., 2004), natural language processing (Jung et al., 1996) and image analysis (Li, 2001). A graphical model is used to display the most significant interactions between random variables. It is thus a quite viable modelling tool for a large variety of real-life datasets. A pertinent example we focus on in this paper is a cell signalling data set collected by Sachs et al. (2005), which consists of 7,466 measurements on 11 phosphorylated proteins involved in primary human immune system cells. Measurements were performed using flow cytometry, which is a popular cell biology technique that produces large samples for measurements of the total amount of proteins. The Bayesian method for colored graphical models selection we develop in this paper allows us to capture the complex pattern of conditional associations and symmetric structures that exist among the proteins.

Højsgaard and Lauritzen (2008) introduce so-called colored graphical models by adding equality constraints on the entries of the correlation matrix \mathbf{R} , or on the entries of the precision matrix \mathbf{K} . In this paper, we will work on the class of colored graphical models obtained by imposing arbitrary equality constraints on \mathbf{K} . Such a model can be represented by a colored graph, where edges or vertices have the same coloring if the corresponding entries of \mathbf{K} are restricted to being identical. Using a colored graphical model typically allows for a reduction in the dimension of the parameter space. Thereby these models can be applied to problems where the number of variables p is substantially larger than the number of observations n .

We now briefly review the various computational methods to perform model selection

in the class of uncolored graphical Gaussian models. Dobra et al. (2011) developed a reversible jump algorithm (Green, 1995). This approach assumes that we can compute the ratio of prior normalizing constants which, in small to moderate dimensions, can be estimated using the Monte Carlo method of Atay-Kayis and Massam (2005). But, as noted by Wang and Li (2012), this approximation cannot be used in high dimensions. Liang (2010) derived a double Metropolis-Hastings sampler, which is an extension of the exchange algorithm (Murray et al., 2006) for simulating from distributions with intractable normalizing constants. This auxiliary variable algorithm avoids the calculation of the normalizing constants altogether and removes the need for exact sampling. Wang and Li (2012) adopted the idea from the double Metropolis-Hasting algorithm to perform graphical Gaussian model selection. Lenkoski (2013) proposed a direct sampler for the G -Wishart distribution and developed a new transdimensional double reversible jump algorithm which integrates the exchange algorithm (Murray et al., 2006) with the reversible jump MCMC (Green, 1995).

To the best of our knowledge, there is no efficient Bayesian method for model selection in the class of colored graphical Gaussian models. When searching this class of models, one is faced with two main problems. One is the efficient computation or estimation of normalizing constants of the colored G -Wishart distribution. The other is the super-exponential growth of the dimension of the colored graph space in p . For example, when p is 4 or 5, the number of uncolored graphs in the space is 64 and 1,024 respectively, whereas the number of colored graphs is 13,155 or 35,285,640 (see Gehrman, 2011).

In this paper, we construct a novel model search procedure which couples linear regression with the double reversible jump scheme. We use linear regression to add significant edges. The model G^* with an additional edge is then compared to the current model G

using the Bayes factor $p(G^*|\mathbf{X})/p(G|\mathbf{X})$ which itself is computed with the help of the double reversible jump MCMC algorithm. The double reversible jump consists of two moves: one move is under the posterior distribution on the state space (G, K) , and the other is an auxiliary move under the prior distribution on the same state space. The double reversible jump algorithm allows for the cancellation of the prior normalizing constants in the expression of the acceptance probability of the chain on (G, K) . We thus avoid computing these quantities which are the usual computational stumbling blocks in graphical Gaussian model selection.

The rest of the paper is organized as follows. Section 2 formally introduces colored graphical models and the colored G -Wishart distribution. Section 3 discusses the model search approach based on linear regression. Section 4 describes our reversible jump MCMC and double reversible jump MCMC algorithms. Section 5 concentrates on the property of model consistency for the proposed model selection algorithm. Section 6 demonstrates the performance of our method through several numerical experiments. Finally, Section 7 presents a real-world application.

2 Preliminaries and notation

We will start by reviewing some of the basic concepts related to colored graphical Gaussian models. For a detailed description, the reader is referred to Højsgaard and Lauritzen (2008) and Massam et al. (2018). We consider an undirected graph $G = (V, E)$ where V is the set of vertices and $E \subset V \times V$ is the set of undirected edges. Let $X = (X_v, v \in V)$ be a random vector following a p -dimensional multivariate normal distribution $N_p(0, \mathbf{K}^{-1})$.

A colored graphical Gaussian model with respect to a colored graph G is constructed

by setting some of the off-diagonal elements of \mathbf{K} to be zero, and some of the diagonal elements or off-diagonal elements of \mathbf{K} to be identical. We say that \mathbf{K} belongs to the cone P_G of symmetric positive definite matrices with zero or equality constraints on the entries of \mathbf{K} . If $K_{v_1, v_2} = 0$ for $(v_1, v_2) \notin E$, then the corresponding variables X_{v_1} and X_{v_2} are conditionally independent giving the remaining variables, which denoted by

$$X_{v_1} \perp\!\!\!\perp X_{v_2} \mid X_{V \setminus \{v_1, v_2\}}.$$

This is called the pairwise Markov property relative to the graph G . If the diagonal elements of \mathbf{K} or the off-diagonal elements are identical, then the corresponding vertices or edges, respectively, are in the same color class. The equality on \mathbf{K} imposes the symmetric structure of the underlying graph G .

The prior distribution on \mathbf{K} is the Diaconis-Ylvisaker conjugate prior for this model and is called as the colored G -Wishart distribution (Massam et al., 2018) defined on P_G and with the density

$$p(\mathbf{K}|\delta, \mathbf{D}, G) = \frac{1}{I_G(\delta, \mathbf{D})} |\mathbf{K}|^{(\delta-2)/2} \exp \left\{ -\frac{1}{2} \langle \mathbf{K}, \mathbf{D} \rangle \right\} \mathbf{1}_{P_G}(\mathbf{K}), \quad (1)$$

where $\delta > 0$, \mathbf{D} is a symmetric positive definite matrix, $\langle \mathbf{A}, \mathbf{B} \rangle$ is the trace inner product, $\mathbf{1}_{P_G}$ is the indicator function of P_G and $I_G(\delta, \mathbf{D})$ is the normalizing constant, namely,

$$I_G(\delta, \mathbf{D}) = \int |\mathbf{K}|^{(\delta-2)/2} \exp \left\{ -\frac{1}{2} \langle \mathbf{K}, \mathbf{D} \rangle \right\} \mathbf{1}_{P_G}(\mathbf{K}) d\mathbf{K}.$$

The goal of the proposed reversible jump MCMC and double reversible jump MCMC is to generate samples from the joint posterior density $p(G, \mathbf{K}|\mathbf{X})$ given the data $\mathbf{X} = (x^1, \dots, x^n)$. The posterior density is

$$\begin{aligned} p(G, \mathbf{K}|\mathbf{X}) &= p(\mathbf{X}|G, \mathbf{K})p(\mathbf{K}|G)p(G) \\ &\propto \frac{1}{I_G(\delta, \mathbf{D})} |\mathbf{K}|^{(n+\delta-2)/2} \exp \left\{ -\frac{1}{2} \langle \mathbf{K}, \mathbf{S} + \mathbf{D} \rangle \right\} p(G) \mathbf{1}_{P_G}(\mathbf{K}), \end{aligned}$$

where $\mathbf{S} = \sum_{i=1}^n (x^i)(x^i)^\top$, and $p(G)$ denotes the prior distribution on the class of graphs considered.

Let $\mathbf{K} = \Phi^\top \Phi$, where $\Phi = (\Phi_{ij})_{1 \leq i \leq j \leq p}$ is an upper triangular matrix with real positive diagonal elements, be the Cholesky decomposition of the matrix \mathbf{K} . Let $\mathcal{V} = \{V_1, \dots, V_t\}$ and $\mathcal{E} = \{E_1, \dots, E_k\}$ denote the set of vertex color classes and edge color classes, respectively. Denote

$$v_u(G) = \min\{(i, j) \in u \mid i \leq j, u \in \mathcal{V} \cup \mathcal{E}\},$$

where the minimum is defined according to the lexicographical order and define

$$v(G) = \bigcup_{u \in \mathcal{V} \cup \mathcal{E}} v_u(G).$$

The vertices and edges $(i, j) \in v(G)$ are called free vertices and free edges, respectively. The remaining vertices and edges are called non-free. Massam et al. (2018) proved that the Jacobian of the change of variables $\mathbf{K}^{v(G)} \rightarrow \Phi^{v(G)}$ is

$$|J(\mathbf{K}^{v(G)} \rightarrow \Phi^{v(G)})| = 2^{|V_G|} \prod_{i=1}^p \Phi_{ii}^{p-i+1-v_i^G}$$

where $|V_G|$ is the number of vertex color classes of G and v_i^G is the number of $j \in \{i, \dots, p\}$ such that $(i, j) \notin v(G)$. Then the posterior distribution of (G, Φ) can be rewritten as

$$\begin{aligned} p(G, \Phi | \mathbf{X}) &= p(\mathbf{X} | G, \mathbf{K}) p(\mathbf{K} | G) |J(\mathbf{K}^{v(G)} \rightarrow \Phi^{v(G)})| p(G) \\ &\propto \frac{2^{|V_G|}}{I_G(\delta, \mathbf{D})} \prod_{i=1}^p \Phi_{ii}^{n+\delta+p-i-1-v_i^G} \exp\left\{-\frac{1}{2} \langle \Phi^\top \Phi, \mathbf{D} + \mathbf{S} \rangle\right\} p(G). \end{aligned} \quad (2)$$

We write $\mathbf{K}^{v(G)} = \{K_{ij} : (i, j) \in v(G)\}$ for the free elements of \mathbf{K} and $\Phi^{v(G)} = \{\Phi_{ij} : (i, j) \in v(G)\}$ for the corresponding free elements of Φ .

3 Algorithm for model selection

As mentioned in the introduction, the number of possible colored graphical models grows exponentially with the number p of variables for a random variable $\mathbf{X} = (X_v, v = 1, \dots, p)$. It is therefore computationally impossible to travel through the space of graphs and compare all models in the space. We thus propose here a new search method for model selection in the class of colored Gaussian graphical models. This method combines linear regression to move from one model to another, with the double reversible jump algorithm to compute the ratio of posterior probabilities of the two models that we compare. Recall that if we partition \mathbf{X} into X_j and $X_{-j} = (X_1, \dots, X_{j-1}, X_{j+1}, \dots, X_p)$, then the conditional distribution of X_j given X_{-j} is Gaussian and the mean $E(X_j | X_{-j})$ is a linear combination of the components of X_{-j} (Hastie et al., 2009; Meinshausen and Bühlmann, 2006).

The algorithm starts with the regression step and then attempts to classify the new edges into color classes. It goes as follows.

Step 1 Start with the graph $G^{[1]}$ with p vertices and no edges. All vertices are free in $G^{[1]}$.

Step 2 Let $G^{[t]}$ be the current graph. Repeat for $j = 1, 2, \dots, p$.

2.a Run the following linear regression to search for potential edges to be added for the graph $G^{[t]}$.

$$X_j \sim \beta_1^j X_1 + \dots + \beta_{j-1}^j X_{j-1} + \beta_{j+1}^j X_{j+1} + \dots + \beta_p^j X_p. \quad (3)$$

Set $\beta_{G^{[t]}}^j = \{\beta_i^j | (i, j) \in G^{[t]}\}$ and find all the significant coefficients β_i^j with p -values less than α in linear regression among $\{\beta_1^j, \dots, \beta_{j-1}^j, \beta_{j+1}^j, \beta_p^j\} \setminus \beta_{G^{[t]}}^j$.

2.b Order the edges from the most significant to the least significant. For each of the edge, we decide whether to accept that edge or not and also determine its color on the basis of the Bayes factor as follows.

2.b.i Let G^* be the graph obtained by adding the edge (i, j) to $G^{[t]}$. Implement model selection between the candidate G^* and the current graph $G^{[t]}$ by estimating the Bayes factor $p(G^*|\mathbf{X})/p(G^{[t]}|\mathbf{X})$ with the help of the double reversible jump algorithm. If the ratio is greater than one, we accept the graph G^* and set $G^{[t+1]} = G^*$. Otherwise, we accept the graph $G^{[t+1]} = G^{[t]}$.

2.b.ii We try to merge the new added edge into the existing color classes. Order the edges in

$$v(G^{[t+1]}) \cap \mathcal{E} = \{u_1, \dots, u_k, k = |v(G^{[t+1]}) \cap \mathcal{E}|\}$$

in the lexicographic order. For $l = 1, \dots, k$,

(α) Let G^{**} be the graph obtained from $G^{[t+1]}$ by setting the the new edge (i, j) accepted (if so) in Step 2.b.i to be in the same class color as u_l . Implement model selection between G^{**} and the current graph $G^{[t+1]}$ by estimating the Bayes factor $p(G^{**}|\mathbf{X})/p(G^{[t+1]}|\mathbf{X})$. If G^{**} is returned, set $G^{[t+2]} = G^{**}$, exit the current color determination step and go back to Step 2.b with the next most significant edge found in Step 2.a.

(β) If (i, j) is not accepted in u_l and $l \neq k$, let $l = l + 1$ and go back to Step 2.b.ii(α).

(γ) If $l = k$ and (i, j) cannot be merged into any of the existing color classes, then (i, j) becomes an additional member of $v(G^{[t+1]}) \cap \mathcal{E}$ and represents a new color class of which it is the only element and the graph remains

$G^{[t+2]} = G^{[t+1]}$. Go back to Step 2.b with the next most significant edge found in Step 2.a.

Step 3 We determine the color classes for all vertices. Start with all vertices free. Repeat for $k = 2, \dots, p$.

3.a Order the vertices in

$$v(G^{[t+2]}) \cap \mathcal{V} = \{u_1, \dots, u_m, m = |v(G^{[t+2]}) \cap \mathcal{V}|\}$$

in the lexicographic order. For $l = 1, \dots, m$,

- (α) Let G^{**} be the graph obtained from $G^{[t+2]}$ by setting the vertex k to be in the same class color as u_l . Compute the Bayes factor $p(G^{**}|\mathbf{X})/p(G^{[t+2]}|\mathbf{X})$ with the help of the double reversible jump algorithm. If the Bayes factor is larger than one, the proposed vertex color merging is accepted, we set $G^{[t+3]} = G^{**}$. We then exit the current color determination step, set $k = k + 1$ and go back to Step 3.
- (β) If the Bayes factor is less than one, we proceed to the next existing vertex color class and let $l = l + 1$.
- (γ) If $l = m$ and vertex k cannot be merged into any existing vertex color class, then $k = (i, i)$ becomes an additional member of $v(G^{[t+2]}) \cap \mathcal{V}$ and represents a new color class of which it is the only element and the graph remains $G^{[t+3]} = G^{[t+2]}$.

The search algorithm above starts with an uncolored graph without any edge and then incrementally adds significant edges by linear regression. Each successful edge addition step is followed by a color determination step for the new edge. The acceptance of a new

model is always decided based on the value of the Bayes factor for the proposed model versus the current model. We illustrate the algorithm on a toy example. Suppose that we have a current graph with two edge color classes in graph G , denoted as red and green in that order. Through linear regression, we add a new edge to the graph. If this new graph is accepted, the new edge is automatically assigned a new color black. Then we try to merge the black edge into the red class first. If accepted, the black edge is changed to a red edge and we consider the next new most significant edge. The current graph has two edge color classes, red and green. If rejected, we then try to merge the black edge into the green class. If accepted, the black edge is changed to a green edge and we consider the next new most significant edge. The current graph still has two edge color classes, red and green. If rejected, the current graph keeps three edge color classes. After considering the edge color classes, we focus on the vertex color classes. We try to merge free vertices into existing color classes. We accept or reject the proposed merge based on the Bayes factor of the proposed new model and the current model. Our algorithm avoids searching through the whole colored graph space, which, as mentioned above, is computationally impossible even for very moderate dimensions.

4 Estimation of Bayes factors

To evaluate Bayes factors such as $p(G^*|\mathbf{X})/p(G^{[t]}|\mathbf{X})$, we aim to simulate a MCMC chain on the posterior distribution of $P(G, \Phi|\mathbf{X})$, where $\mathbf{K} = (\Phi)^\top \Phi$ follows the colored G -Wishart distribution $CW_G(\delta + n, \mathbf{D} + \mathbf{S})$. We sample G from the two neighboring colored graphs $\{G^*, G^{[t]}\}$ and each graph is assumed to have equal prior. Based on this sampling of G from the simulated posterior distribution, we count the proportion of samples belonging to graph

G^* and $G^{[t]}$ respectively as the empirical estimates of their marginal posterior distributions $P(G^*|\mathbf{X})$ and $P(G^{[t]}|\mathbf{X})$. Then we estimate the Bayes factor based on these proportions. We extend the ideas from the reversible jump MCMC (Dobra et al., 2011) and the double reversible jump (Lenkoski, 2013) for uncolored graphical models to the colored graphical models and colored G -Wishart distribution.

Given a colored graph G , a neighbor of G is a graph obtained by deleting or adding one edge in G , or a graph obtained by deleting or adding one vertex color class or one edge color class. Here deleting a color class means that an entry (i, j) that was previously free becomes a non-free one, that is, it joins an existing color class $u \in \mathcal{V} \cup \mathcal{E}$. Adding a color class means that an entry (i, j) that belonged to a color class $u \in \mathcal{V} \cup \mathcal{E}$ becomes free, creating a color class of its own and thus increasing the cardinality of $\mathcal{V} \cup \mathcal{E}$. The chain moves between two neighboring colored graphs which are in two different dimensions of the parameter space.

4.1 Reversible jump MCMC

We describe a reversible jump sampler based on a colored G -Wishart prior for \mathbf{K} . This approach requires the calculation of the normalizing constants of the G -Wishart priors corresponding to the current and the candidate graphs. It can thus be used only for some small specific graphs for which we can compute the normalizing constants. Let us, now, present the details of the reversible jump algorithm for different cases. We denote the current state of the chain by $(\mathbf{K}^{[t]}, G^{[t]})$ and the next state by $(\mathbf{K}^{[t+1]}, G^{[t+1]})$. For a given colored graph $G^{[t]}$, we make use of the Monte Carlo method of Massam et al. (2018) to obtain the samples $\mathbf{K}^{[t]}$ from the colored G -Wishart distribution. Let G^* be the candidate colored graph. Let $\mathbf{K}^{[t]} = (\Phi^{[t]})^\top \Phi^{[t]}$ and $\mathbf{K}^* = (\Phi^*)^\top \Phi^*$ be the respective Cholesky

decomposition of the precision matrices. We update one entry of Φ at a time. All the non-updated free elements of $\Phi^{[t]}$ coincide with the corresponding ones of Φ^* . The non-free elements of Φ^* are determined through the completion operation by Proposition 1 in Massam et al. (2018).

Case 1. The candidate G^* is obtained by changing the non-free edge (i, j) of $G^{[t]}$ to a free one. We consider two different scenarios. In the first scenario, G^* is obtained by adding the edge (i, j) on $G^{[t]}$. In the second scenario, G^* is obtained by removing a color constraint on the edge (i, j) . For both scenarios, we sample $\gamma \sim N(\Phi_{ij}^{[t]}, \sigma)$ which is a proposal distribution for the updated Φ_{ij}^* and set $\Phi_{ij}^* = \gamma$. The Markov chain moves to (G^*, \mathbf{K}^*) with probability $\min\{R_0^+, 1\}$ where R_0^+ is

$$\begin{aligned} & \frac{p(G^*, \Phi^* | \mathbf{X})}{p(G^{[t]}, \Phi^{[t]} | \mathbf{X})} * \frac{1}{\frac{1}{\sqrt{2\pi}\sigma} \exp\{-\frac{1}{2\sigma^2}(\Phi_{ij}^* - \Phi_{ij}^{[t]})^2\}} \\ &= \frac{\frac{2^{|V_{G^*}|}}{I_{G^*}(\delta, \mathbf{D})} \prod_{i=1}^p (\Phi_{ii}^*)^{n+\delta+p-i-1-v_i^{G^*}} \exp\{-\frac{1}{2} \langle (\Phi^*)^\top \Phi^*, \mathbf{D} + \mathbf{S} \rangle\} p(G^*)}{\frac{2^{|V_{G^{[t]}}|}}{I_{G^{[t]}}(\delta, \mathbf{D})} \prod_{i=1}^p (\Phi_{ii}^{[t]})^{n+\delta+p-i-1-v_i^{G^{[t]}}} \exp\{-\frac{1}{2} \langle (\Phi^{[t]})^\top \Phi^{[t]}, \mathbf{D} + \mathbf{S} \rangle\} p(G^{[t]})} \\ & \quad * \frac{\sqrt{2\pi}\sigma}{\exp\{-\frac{1}{2\sigma^2}(\Phi_{ij}^* - \Phi_{ij}^{[t]})^2\}}. \end{aligned}$$

Case 2. The candidate G^* is obtained by changing the non-free vertex (i, i) on $G^{[t]}$ to a free one. We sample γ from a proposal distribution $N^+(\Phi_{ii}^{[t]}; \sigma, 0, \infty)$ which is the normal distribution truncated below at zero, with mean $\Phi_{ii}^{[t]}$ and set $\Phi_{ii}^* = \gamma$. The Markov chain moves to (G^*, \mathbf{K}^*) with probability $\min\{R_v^+, 1\}$ where R_v^+ is

$$\frac{\frac{2^{|V_{G^*}|}}{I_{G^*}(\delta, \mathbf{D})} \prod_{i=1}^p (\Phi_{ii}^*)^{n+\delta+p-i-1-v_i^{G^*}} \exp\{-\frac{1}{2} \langle (\Phi^*)^\top \Phi^*, \mathbf{D} + \mathbf{S} \rangle\} p(G^*)}{\frac{2^{|V_{G^{[t]}}|}}{I_{G^{[t]}}(\delta, \mathbf{D})} \prod_{i=1}^p (\Phi_{ii}^{[t]})^{n+\delta+p-i-1-v_i^{G^{[t]}}} \exp\{-\frac{1}{2} \langle (\Phi^{[t]})^\top \Phi^{[t]}, \mathbf{D} + \mathbf{S} \rangle\} p(G^{[t]})} * \frac{1}{f(\Phi_{ii}^*; \Phi_{ii}^{[t]}, \sigma, 0, +\infty)}$$

where $f(*; \mu, \sigma, 0, +\infty)$ is the density function for the truncated normal distribution.

4.2 Double reversible jump MCMC

The reversible jump MCMC in subsection 4.1 assumes that we can compute the normalizing constants $I_G(\delta, \mathbf{D})$. In Section 6, we compute the normalizing constant of some specific colored graphs. But, in general, we do not know how to obtain the analytic expression of these constants or even how to estimate them efficiently. To circumvent this problem, we will use the double reversible jump MCMC algorithm which avoids the calculation of the normalizing constants.

We sample from the posterior distribution $p(G, \Phi | \mathbf{X})$, where $\mathbf{K} = (\Phi)^\top \Phi$ follows the colored G -Wishart distribution $CW_G(\delta + n, \mathbf{D} + \mathbf{S})$. Then we introduce the auxiliary variables \tilde{G} and Ω , which share the same state spaces as G and Φ , and the positive definite matrix $\Psi = (\Omega)^\top \Omega$ which follows the colored G -Wishart distribution $CW_{\tilde{G}}(\delta, \mathbf{D})$.

We can simulate $(G, \Phi, \tilde{G}, \Omega)$ as follows:

Case 1: If G^* is obtained by adding one edge (i, j) to the current graph $G^{[t]}$. Let $G_1 = G^{[t]}$ and $G_2 = G^*$.

- 1.1 Sample $\mathbf{K}^{[t]} \sim CW_{G_1}(\delta + n, \mathbf{D} + \mathbf{S})$ with $\mathbf{K}^{[t]} = (\Phi^{[t]})^\top \Phi^{[t]}$ using the Monte Carlo method of Massam et al. (2018).
- 1.2 Sample $\Phi_{ij}^* \sim N(\Phi_{ij}^{[t]}, \sigma)$, which is the proposal distribution of the updated Φ_{ij}^* with an arbitrary σ . Let all free elements in Φ^* take the same values as in $\Phi^{[t]}$ except for Φ_{ij}^* .
- 1.3 Sample $\Psi^{[t]} = (\Omega^{[t]})^\top \Omega^{[t]}$ from $CW_{G_2}(\delta, \mathbf{D})$ using the Monte Carlo method of Massam et al. (2018).
- 1.4 Let the free elements in Ω^* take the same values as in $\Omega^{[t]}$ except for Ω_{ij}^* and

$$\Omega_{ij}^* = \begin{cases} 0 & \text{if } i = 1 \\ -\frac{\sum_{k=1}^{i-1} \Omega_{ki}^{[t]} \Omega_{kj}^{[t]}}{\Omega_{ii}^{[t]}} & \text{otherwise.} \end{cases}$$

1.5 Accept the move from $(G^{[t]}, \Phi^{[t]}, \tilde{G}^{[t]}, \Omega^{[t]})$ to $(G^*, \Phi^*, \tilde{G}^*, \Omega^*)$ with probability $\min\{1, r_0^+\}$ where

$$r_0^+ = \frac{\prod_{i=1}^p (\Phi_{ii}^*)^{n+\delta+p-i-1-v_i^{G_2}} \exp\{-\frac{1}{2}\langle(\Phi^*)^\top \Phi^*, \mathbf{D}+\mathbf{S}\rangle\}}{\prod_{i=1}^p (\Phi_{ii}^{[t]})^{n+\delta+p-i-1-v_i^{G_1}} \exp\{-\frac{1}{2}\langle(\Phi^{[t]})^\top \Phi^{[t]}, \mathbf{D}+\mathbf{S}\rangle\}} * \frac{1}{\exp\{-\frac{1}{2\sigma^2}(\Phi_{ij}^* - \Phi_{ij}^{[t]})^2\}}$$

$$= \frac{\prod_{i=1}^p (\Omega_{ii}^{[t]})^{\delta+p-i-1-v_i^{G_2}} \exp\{-\frac{1}{2}\langle(\Omega^{[t]})^\top \Omega^{[t]}, \mathbf{D}\rangle\}}{\prod_{i=1}^p (\Omega_{ii}^*)^{\delta+p-i-1-v_i^{G_1}} \exp\{-\frac{1}{2}\langle(\Omega^*)^\top \Omega^*, \mathbf{D}\rangle\}} * \frac{1}{\exp\{-\frac{1}{2\sigma^2}(\Omega_{ij}^{[t]} - \Omega_{ij}^*)^2\}}$$

The term in the numerator is for moving from $(G_1, \Phi^{[t]})$ to (G_2, Φ^*) where $\Phi^{[t]}$ and Φ^* follow the posterior distribution. The term in the denominator is for moving from $(G_2, \Omega^{[t]})$ to (G_1, Ω^*) where $\Omega^{[t]}$ and Ω^* follow the prior distribution.

Case 2: If G^* is obtained by changing one non-free edge (i, j) to a free edge from $G^{[t]}$ or, equivalently by adding one edge color class in $G^{[t]}$. Steps 2.1–2.3 and 2.5 are the same with those in Case 1.

2.4. Let the free elements in Ω^* take the same values as in $\Omega^{[t]}$ except for Ω_{ij}^* and

$$\Omega_{ij}^* = \frac{\Omega_{i_u j_u}^{[t]} \Omega_{i_u i_u}^{[t]} + \sum_{k=1}^{i_u-1} \Omega_{k i_u}^{[t]} \Omega_{k j_u}^{[t]} - \sum_{k=1}^{i-1} \Omega_{k i}^{[t]} \Omega_{k j}^{[t]}}{\Omega_{ii}^{[t]}},$$

where $u \in \mathcal{V} \cup \mathcal{E}$, $(i_u, j_u) = \min\{(i, j) \in u : i \leq j\}$ in the lexicographical order.

Case 3: If G^* is obtained by changing one non-free vertex (i, i) to a free vertex from $G^{[t]}$ or, equivalently adding one vertex color class in $G^{[t]}$. Steps 3.1 and 3.3 are the same as Steps 1.1 and 1.3.

3.2 Sample Φ_{ii}^* from the proposal distribution $f(\Phi_{ii}^*; \Phi_{ii}^{[t]}, \sigma, 0, +\infty)$, the normal distribution truncated below at zero, and let the free $\Phi^* = \Phi^{[t]}$ except for Φ_{ii}^* .

3.4 Let the free elements in Ω^* take the same values as in $\Omega^{[t]}$ except for Ω_{ii}^* and

$$\Omega_{ii}^* = |(\Omega_{i_u i_u}^{[t]})^2 + \sum_{k=1}^{i_u-1} (\Omega_{k i_u}^{[t]})^2 - \sum_{k=1}^{i-1} (\Omega_{k i}^{[t]})^2|^{\frac{1}{2}}.$$

3.5 Accept the move from $(G^{[t]}, \Phi^{[t]}, \tilde{G}^{[t]}, \Omega^{[t]})$ to $(G^*, \Phi^*, \tilde{G}^*, \Omega^*)$ with probability $\min\{1, r_v^+\}$ where

$$r_v^+ = \frac{\prod_{i=1}^p (\Phi_{ii}^*)^{n+\delta+p-i-1-v_i^{G_2}} \exp\{-\frac{1}{2}\langle(\Phi^*)^\top \Phi^*, \mathbf{D}+\mathbf{S}\rangle\}}{\prod_{i=1}^p (\Phi_{ii}^{[t]})^{n+\delta+p-i-1-v_i^{G_1}} \exp\{-\frac{1}{2}\langle(\Phi^{[t]})^\top \Phi^{[t]}, \mathbf{D}+\mathbf{S}\rangle\}} * \frac{1}{f(\Phi_{ii}^*; \Phi_{ii}^{[t]}, \sigma, 0, +\infty)}$$

$$= \frac{\prod_{i=1}^p (\Omega_{ii}^{[t]})^{\delta+p-i-1-v_i^{G_2}} \exp\{-\frac{1}{2}\langle(\Omega^{[t]})^\top \Omega^{[t]}, \mathbf{D}\rangle\}}{\prod_{i=1}^p (\Omega_{ii}^*)^{\delta+p-i-1-v_i^{G_1}} \exp\{-\frac{1}{2}\langle(\Omega^*)^\top \Omega^*, \mathbf{D}\rangle\}} * \frac{1}{f(\Omega_{ii}^{[t]}; \Omega_{ii}^*, \sigma, 0, +\infty)}.$$

5 Model selection consistency

Denote G_T as the true graph that generates the data \mathbf{X} , and G_s as any competitor graph that can be used to model \mathbf{X} . In this section, we are going to show that, as the sample size increases, the probability that the Bayes factor selects the true graph G_T over the competitor graph G_s converges to one.

The competitor graphs fall into two categories: an underfitting graph, denoted by G_- with missing edges or incorrect partitions of the edges into different color classes and an overfitting graph denoted by G_+ with more edges or finer partitions of the color classes. The true graph G_T contains the edge set E_T , the edge color classes E_1^T, \dots, E_k^T and the vertices color classes V_1^T, \dots, V_t^T . The competitor graph G_s contains the edge set E_s , the edge color classes E_1^s, \dots, E_k^s and the vertices color classes V_1^s, \dots, V_t^s . If the following three conditions are satisfied and $G_s \neq G_T$, then the graph G_s is called an overfitting graph denoted by G_+ . Any other competitor graph is called an underfitting graph which is denoted by G_- .

1. $E_T \subseteq E_s$.
2. For any edge class $E_i^s, i \in \{1, \dots, k^s\}$ in G^s , there exists a edge class $E_j^T, j \in \{1, \dots, k\}$ in G^T such that

$$E_i^s \cap E_T \subseteq E_j^T.$$

3. For any vertex class $V_i^s, i \in \{1, \dots, t^s\}$ in G^s , there exists a vertex class $V_j^T, j \in \{1, \dots, t\}$ in G^T such that

$$V_i^s \subseteq V_j^T.$$

Denote d_G as the number of parameters in the colored graphical model with underlying graph G , i.e., the total number of edge classes and vertex classes. Then by the definition above, $d_{G_+} > d_{G_T}$. The following theorem demonstrates that, as the sample size n tends to infinity, the Bayes factor is model selection consistent for colored Gaussian graphical models.

Theorem 5.1 *Consider a colored graphical model where the number of vertices in the underlying graph is finite. Let G_T be the true graph and let G_s be any competing graph, then*

$$\lim_{n \rightarrow \infty} p_T \left(p(G_T | \mathbf{X}) > p(G_s | \mathbf{X}) \right) = 1.$$

Theorem 5.1 states that, under the true model G_T , the probability that the Bayes factor for the true model G_T versus any other model G be greater than one, tends to one as the sample size increases. At each step of our procedure, we move from one graph $G^{[t]}$ to another graph G^* if and only if the Bayes factor for G^* versus $G^{[t]}$ is greater than one. So, though we cannot guarantee that our procedure converges to the true graph G_T , we see that it moves towards the true graph.

If sample size goes to infinity and we use Bayes factor to compare all candidate models, we will be able to find the true model with probability tending to one. However due to the astronomical size of the model space, we cannot evaluate and compare all possible models. Thus our hill climbing algorithm is a practical strategy to search through the model space.

6 Numerical experiments

In subsection 6.1 below, we compare the performance of the proposed reversible jump algorithm and the double reversible jump algorithm to evaluate the Bayes factors. The values obtained are compared to the true values of the Bayes factor which, in the case of the small graphs that we consider, can be computed analytically and thus exactly numerically. In subsection 6.2, we analyze the validity of the proposed model selection approach based on the double reversible jump algorithm.

For the prior G -Wishart distribution, the hyperparameters are $\delta = 3$ and $\mathbf{D} = \mathbf{I}$, the identity matrix. We use $\sigma = 0.5$ to generate the samples from the normal distributions and truncated normal distributions. We implement all algorithms in R.

6.1 Estimation of Bayes factors

6.1.1 Graph with 3 vertices

This simulation experiment is designed to assess the accuracy of the estimates of Bayes factors produced by our proposed samplers. Since in the case of graphs with three vertices, we can compute the normalizing constant of the G -Wishart distribution. We empirically compare the estimates of Bayes factors using the reversible jump MCMC (RJ), the double reversible jump MCMC (DRJ), and the theoretical value of the ratio of normalizing constants (RN). For two neighboring colored graphs G_1 and G_2 , the RN is defined by

$$RN = \frac{\frac{I_{G_1}(\delta+n, \mathbf{D}+\mathbf{S})}{I_{G_1}(\delta, \mathbf{D})}}{\frac{I_{G_2}(\delta+n, \mathbf{D}+\mathbf{S})}{I_{G_2}(\delta, \mathbf{D})}}.$$

We consider different colored graphs with three vertices in Figure 1 for which we can compute the corresponding normalizing constants exactly. The normalizing constants of colored G -Wishart distributions for the five colored graphs shown in Figure 1 can be computed using Theorems

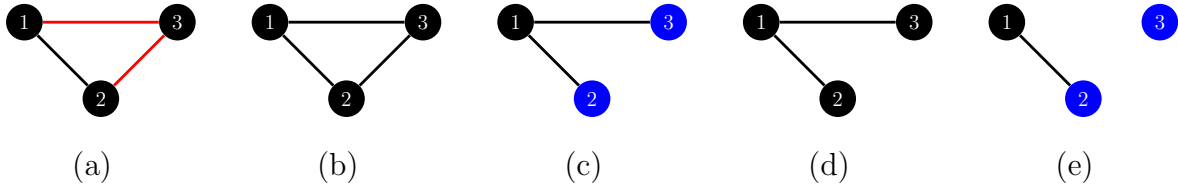


Figure 1: Colored graphs with 3 vertices.

3 and 5 in Massam et al. (2018), Theorems 6.1, and the formula in Atay-Kayis and Massam (2005). We generate one dataset comprising $n = 100$ observations sampled from the multivariate normal $N(0, \mathbf{K}^{-1})$. The two MCMC samplers are run for 10,000 iterations with a burn-in of 1000 iterations. Computational results are summarized in Tables 1, 2 and 3. Results indicate that the double reversible jump MCMC can produce almost the same accuracy as the reversible jump MCMC. Estimates from both algorithms perform very well when compared with the theoretical values of Bayes factors.

The following theorem gives the analytic expression of the normalizing constants for the colored G -Wishart distributions with underlying graph as shown in Figure 1 (e).

Theorem 6.1 *For the colored graph G of Figure 1 (e), the normalizing constant $I_G(\delta, \mathbf{D})$ is*

$$I_G(\delta, \mathbf{D}) = \frac{2^{\frac{\delta+1}{2}} \Gamma(\frac{\delta}{2}) \sqrt{\pi} d_{11}^{-\frac{\delta+1}{2}} \Gamma(\delta - \frac{1}{2})}{[\frac{1}{2}(d_{22} + d_{33}) - \frac{d_{12}^2}{2d_{11}}]^{\delta - \frac{1}{2}}},$$

where $\mathbf{D} = (d_{ij})_{1 \leq i, j \leq p}$.

The proof of Theorem 6.1 is given in the Appendix.

6.1.2 Star graphs with 8 vertices

We consider two star graphs with $p = 8$ in Figure 2. The normalizing constants of colored G -Wishart distributions underlying the graphs in Figure 2 (a) and (b) are computed by Theorems

Table 1: Estimation of Bayes factors for Figure 1 (c) vs. Figure 1 (e). Standard errors are indicated in parentheses.

K	$\begin{pmatrix} 1 & 0.4 & 0.2 \\ 0.4 & 1 & 0 \\ 0.2 & 0 & 1 \end{pmatrix}$	$\begin{pmatrix} 1 & 0.4 & 0.22 \\ 0.4 & 1 & 0 \\ 0.22 & 0 & 1 \end{pmatrix}$	$\begin{pmatrix} 1 & 0.4 & 0 \\ 0.4 & 1 & 0 \\ 0 & 0 & 1 \end{pmatrix}$	$\begin{pmatrix} 1 & 0.4 & 0.1 \\ 0.4 & 1 & 0 \\ 0.1 & 0 & 1 \end{pmatrix}$
RJ	2.167 (0.122)	2.916 (0.084)	0.237 (0.005)	1.445 (0.034)
DRJ	2.114 (0.055)	3.314 (0.167)	0.242 (0.009)	1.481 (0.051)
RN	2.181	3.017	0.234	1.469

Table 2: Estimation of Bayes factors for Figure 1 (b) vs. Figure 1 (a). Standard errors are indicated in parentheses.

K	$\begin{pmatrix} 1 & 0.4 & 0.2 \\ 0.4 & 1 & 0 \\ 0.2 & 0 & 1 \end{pmatrix}$	$\begin{pmatrix} 1 & 0.4 & 0.38 \\ 0.4 & 1 & 0 \\ 0.38 & 0 & 1 \end{pmatrix}$	$\begin{pmatrix} 1 & 0.4 & 0 \\ 0.4 & 1 & 0 \\ 0 & 0 & 1 \end{pmatrix}$	$\begin{pmatrix} 1 & 0.4 & 0.1 \\ 0.4 & 1 & 0 \\ 0.1 & 0 & 1 \end{pmatrix}$
RJ	3.953 (0.327)	6.053 (0.648)	0.151 (0.004)	0.229 (0.007)
DRJ	4.217 (0.410)	5.782 (0.580)	0.149 (0.006)	0.227 (0.013)
RN	4.349	5.511	0.152	0.229

Table 3: Estimation of Bayes factors for Figure 1 (d) vs. Figure 1 (c). Standard errors are indicated in parentheses.

\mathbf{K}	$\begin{pmatrix} 1 & 0.4 & 0.2 \\ 0.4 & 1 & 0 \\ 0.2 & 0 & 1 \end{pmatrix}$	$\begin{pmatrix} 1 & 0.4 & 0.2 \\ 0.4 & 1.35 & 0 \\ 0.2 & 0 & 1 \end{pmatrix}$	$\begin{pmatrix} 1 & 0.4 & 0.2 \\ 0.4 & 1.2 & 0 \\ 0.2 & 0 & 1 \end{pmatrix}$	$\begin{pmatrix} 1 & 0.4 & 0.2 \\ 0.4 & 1 & 0 \\ 0.2 & 0 & 1.1 \end{pmatrix}$
RJ	0.112 (0.004)	1.793 (0.078)	0.568 (0.030)	0.413 (0.013)
DRJ	0.105 (0.006)	1.708 (0.116)	0.545 (0.025)	0.402 (0.019)
RN	0.109	1.988	0.480	0.388

Table 4: Estimation of Bayes factors for Figure 2 (a) vs. Figure 2 (b). Standard errors are indicated in parentheses.

K_{pp}	1	1.2	1.3	1.4
RJ	0.004 (0.001)	0.020 (0.002)	0.057 (0.005)	0.255 (0.026)
DRJ	0.008 (0.001)	0.020 (0.005)	0.051 (0.009)	0.199 (0.034)
RN	0.004	0.019	0.063	0.230

3 and 4 in Massam et al. (2018), respectively. Following Wang and Li (2012), we construct $\mathbf{S} = n\mathbf{K}^{-1}$ which corresponds to $n = 100$ independent observations of $N(0, \mathbf{K}^{-1})$. Furthermore, the precision matrix \mathbf{K} is given by $K_{ii} = 1$ for $i = 1, \dots, p - 1$ and $K_{pj} = K_{jp} = 0.3$ for $j = 1, \dots, p - 1$. The element K_{pp} corresponding to the center of star graphs is shown in Table 4. To evaluate the performance of RJ and DRJ algorithms, we run these algorithms with 10000 iterations and 1000 as a burn-in. Table 4 reports comparisons of our methods with the true values of the Bayes factors.

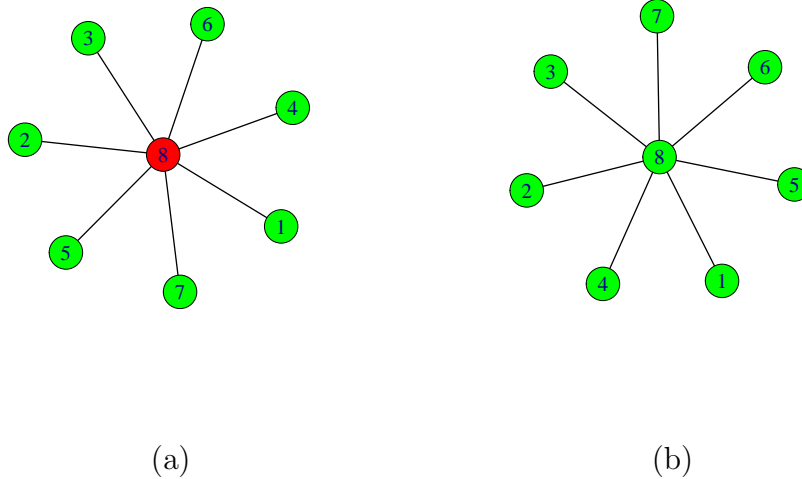


Figure 2: Two star graphs with 8 vertices.

6.2 Model selection

We conduct model selection experiments using the algorithm proposed in Section 3. The double reversible jump MCMC algorithm is used to estimate the Bayes factors and the sampler is run for 5,000 iterations with a burn-in of 1000 iterations. The threshold for the linear regression step of our method is $\alpha = 0,05$.

6.2.1 Graphs with three vertices

We simulate 50 datasets each comprising $n = 100$ observations sampled from multivariate normal $N(0, \mathbf{K}^{-1})$. Tables 5, 6 and 7 show the average edge inclusion probabilities and percentages of the true graphical structure produced from the model selection algorithm. Our algorithm recovers the true graphical structure for different colored graphs very well: true colored models are selected with probabilities above 0.82. The edges that should belong to the true graph receive inclusion probabilities above 0.90, while the edges that should be absent from the true graph

Table 5: The percentages of the true model being selected over 50 simulated datasets, edge inclusion probabilities (IP) and timing (in seconds) for the algorithm of model selection.

K	$\begin{pmatrix} 1 & 0.4 & 0.4 \\ 0.4 & 1 & 0 \\ 0.4 & 0 & 1 \end{pmatrix}$	$\begin{pmatrix} 1 & 0.5 & 0.5 \\ 0.5 & 2 & 0 \\ 0.5 & 0 & 1 \end{pmatrix}$	$\begin{pmatrix} 1 & 0.4 & 0 \\ 0.4 & 0.5 & 0.4 \\ 0 & 0.4 & 0.5 \end{pmatrix}$
IP	$\begin{pmatrix} * & 0.98 & 0.98 \\ * & * & 0.02 \\ * & * & * \end{pmatrix}$	$\begin{pmatrix} * & 1 & 1 \\ * & * & 0.1 \\ * & * & * \end{pmatrix}$	$\begin{pmatrix} * & 1 & 0 \\ * & * & 1 \\ * & * & * \end{pmatrix}$
Percentage	0.98	0.88	1
Timing	261.36	316.06	277.71

receive inclusion probabilities below 0.08. The CPU time (in seconds) for one dataset is also given in Tables 5, 6 and 7.

6.2.2 Star graphs with $p=8$ vertices and $p=11$ vertices

Let \mathbf{K}^T and $\hat{\mathbf{K}}$ be the true precision matrix and the precision matrix selected through the model selection approach, respectively. To assess the performance of the symmetric structure, we compute the measures d_0 , $d_{V_i^T}$, $i = 1, \dots, t$, $d_{E_j^T}$, $j = 1, \dots, k$, and Acc_{all} defined below for measuring supervised clustering and feature selection in Shen et al. (2012). Let B be the set of missing edges in the true graph, i.e. such that $K_{ij}^T = 0$.

We define

$$d_0 = \left\{ \sum_{(i,j) \in B} \mathbf{1}_{\hat{K}_{ij}=0} + \sum_{(i,j) \notin B} \mathbf{1}_{\hat{K}_{ij} \neq 0} \right\} / \frac{p(p-1)}{2}$$

Table 6: The percentages of the true model being selected over 50 simulated datasets, edge inclusion probabilities (IP) and timing (in seconds) for the algorithm of model selection.

K	$\begin{pmatrix} 1 & 0.4 & 0.4 \\ 0.4 & 1 & 0.4 \\ 0.4 & 0.4 & 1 \end{pmatrix}$	$\begin{pmatrix} 1.5 & 1 & 1 \\ 1 & 1 & 0 \\ 1 & 0 & 3 \end{pmatrix}$	$\begin{pmatrix} 1 & 0.5 & 1.5 \\ 0.5 & 0.5 & 0 \\ 1.5 & 0 & 3 \end{pmatrix}$
IP	$\begin{pmatrix} * & 1 & 0.94 \\ * & * & 0.98 \\ * & * & * \end{pmatrix}$	$\begin{pmatrix} * & 1 & 1 \\ * & * & 0 \\ * & * & * \end{pmatrix}$	$\begin{pmatrix} * & 0.06 & 1 \\ * & * & 0.08 \\ * & * & * \end{pmatrix}$
Percentage	0.82	0.98	1
Timing	346.64	308.56	211.42

Table 7: The percentages of the true model being selected over 50 simulated datasets, edge inclusion probabilities (IP) and timing (in seconds) for the algorithm of model selection.

K	$\begin{pmatrix} 0.5 & 0 & 0 \\ 0 & 2 & 0 \\ 0 & 0 & 0.5 \end{pmatrix}$	$\begin{pmatrix} 0.5 & 0 & 0 \\ 0 & 0.5 & 0 \\ 0 & 0 & 0.5 \end{pmatrix}$	$\begin{pmatrix} 1.5 & 0.6 & 0 \\ 0.6 & 2 & 1.4 \\ 0 & 1.4 & 1.5 \end{pmatrix}$
IP	$\begin{pmatrix} * & 0.08 & 0.06 \\ * & * & 0.06 \\ * & * & * \end{pmatrix}$	$\begin{pmatrix} * & 0.06 & 0.06 \\ * & * & 0.04 \\ * & * & * \end{pmatrix}$	$\begin{pmatrix} * & 0.9 & 0.06 \\ * & * & 1 \\ * & * & * \end{pmatrix}$
Percentage	0.84	0.86	0.84
Timing	346.64	308.56	211.42

concerning the zero constraints. For $i = 1, \dots, t$, let

$$d_{V_i^T} = \frac{\sum_{j \neq j': (j,j) \in V_i^T, (j',j') \in V_i^T} \mathbf{1}_{\hat{K}_{jj} = \hat{K}_{j'j'}} + \sum_{j \neq j': (j,j) \in V_i^T, (j',j') \notin V_i^T} \mathbf{1}_{\hat{K}_{jj} \neq \hat{K}_{j'j'}}}{|V_i^T|(p-1)}$$

which measures the performance in identifying the true vertex color classes. For $j = 1, \dots, k$, let

$$d_{E_j^T} = \frac{\sum_{\substack{(k,l) \neq (k',l'): \\ (k,l) \in E_j^T, \\ (k',l') \in E_j^T}} \mathbf{1}_{\hat{K}_{kl} = \hat{K}_{k'l'}} + \sum_{\substack{(k,l) \neq (k',l'): \\ (k,l) \in E_j^T, \\ (k',l') \notin E_j^T}} \mathbf{1}_{\hat{K}_{kl} \neq \hat{K}_{k'l'}}}{|E_j^T| \left[\binom{p-1}{2} - 1 \right]}$$

which measures the performance in identifying the true edge color classes. We further define

$$Acc_{all} = \frac{d_0 + \sum_{i=1}^s d_{V_i^T} + \sum_{j=1}^t d_{E_j^T}}{1 + s + t}.$$

Note that Acc_{all} lies between 0 and 1. The bigger Acc_{all} is, the better performance is.

We simulate 20 datasets each comprising $n = 1000$ observations sampled from multivariate normal $N(0, (\mathbf{K}^T)^{-1})$ where $K_{ii}^T = 1$, $K_{ip}^T = K_{pi}^T = 0.3$, for $i = 1, 2, \dots, p$, and $K_{ij}^T = 0$ for others.

For $p = 8$ and $p = 11$, the average edge inclusion probabilities over 20 simulated datasets are

$$IP = \begin{pmatrix} * & 0.05 & 0.15 & 0.05 & 0.05 & 0.05 & 0.05 & 1 \\ & * & 0 & 0.05 & 0 & 0 & 0 & 1 \\ & & * & 0.1 & 0 & 0 & 0 & 1 \\ & & & * & 0.05 & 0 & 0.05 & 0.95 \\ & & & & * & 0 & 0.05 & 1 \\ & & & & & * & 0.05 & 1 \\ & & & & & & * & 1 \\ & & & & & & & * \end{pmatrix}$$

Table 8: Measures for star graphs when $p = 8$ and $p = 11$. Standard errors are indicated in parentheses.

	\bar{d}_0	\bar{d}_{V_1}	\bar{d}_{E_1}	\overline{Acc}_{all}
$p = 8$	0.971(0.021)	0.879(0.164)	0.967(0.056)	0.940(0.066)
$p = 11$	0.947(0.033)	0.383(0.222)	0.835(0.063)	0.722(0.103)

and

$$IP = \begin{pmatrix} * & 0 & 0.1 & 0.05 & 0.2 & 0.1 & 0.05 & 0 & 0 & 0.05 & 1 \\ & * & 0.15 & 0 & 0.05 & 0.1 & 0.05 & 0 & 0 & 0.05 & 1 \\ & & * & 0.05 & 0 & 0.05 & 0.05 & 0 & 0.05 & 0 & 0.9 \\ & & & * & 0 & 0.1 & 0 & 0.05 & 0 & 0 & 0.9 \\ & & & & * & 0 & 0.05 & 0.1 & 0.1 & 0.05 & 0.85 \\ & & & & & * & 0 & 0.05 & 0.1 & 0 & 0.85 \\ & & & & & & * & 0 & 0.1 & 0 & 0.85 \\ & & & & & & & * & 0 & 0 & 0.9 \\ & & & & & & & & * & 0 & 0.75 \\ & & & & & & & & & * & 0.95 \\ & & & & & & & & & & * \end{pmatrix},$$

respectively. The values for measuring the symmetric structure are shown in Table 8.

7 Application to flow cytometry data

We analyze a flow cytometry dataset on signaling networks of human immune system cells. Flow cytometry can measure multiple molecules within each cell and it is possible to identify complex causal influence relationships involving multiple proteins (Sachs et al., 2005). Sachs et al. (2005) fitted a directed acyclic graph to depict the signalling pathway between the proteins. Using the

fractional pseudo-likelihood method, Leppä-aho et al. (2017) analyzed interactions between the proteins based on the uncolored and undirected graphs. The dataset includes $p = 11$ proteins and $n = 7466$ observations.

We want to detect the underlying colored graph for the flow cytometry data using the proposed model selection algorithm in Section 3. Even with a moderate number of variables $p = 11$, the model space for colored graphical models is astronomical in size. In order to speed up the model search approach, we add a likelihood ratio test (Højsgaard and Lauritzen, 2008) before using Bayes factors estimation between two colored graphs. When comparing a colored graph G_1 with a candidate graph G_2 obtained by adding one edge or deleting one vertex color class on G_1 , we compute a likelihood ratio on one degree of freedom using the R function `rcox()` in the R package `gRc` (Højsgaard and Lauritzen, 2007). If the candidate graph G_2 is not selected using the likelihood ratio test, we will not consider G_2 in the model selection algorithm.

In the model selection procedure, we set $\delta = 3$, $\sigma = 0.5$ and \mathbf{D} be the identity matrix. Further, we run the double reversible jump algorithm for 10,000 iterations and discard the first 1,000 as burn-in. The best colored graph selected through our model selection algorithm is presented in Figure 3. The selected graph contains 27 edges, 24 edge color classes and 11 vertex color classes. There are 18 edges in common with the edges in the uncolored graph developed in Leppä-aho et al. (2017), which has 31 edges in total. Comparing with the results of Leppä-aho et al. (2017), we detect many common edges and those warrant future biological validations. Our method has the advantage of detecting symmetries in the graphical model and in this particular case, we find that there are in fact only few symmetries in the graph.

8 Concluding remarks

We propose a Bayesian method to perform model selection in the class of colored Gaussian graphical models which allows us to capture the symmetric structure and dependency patterns

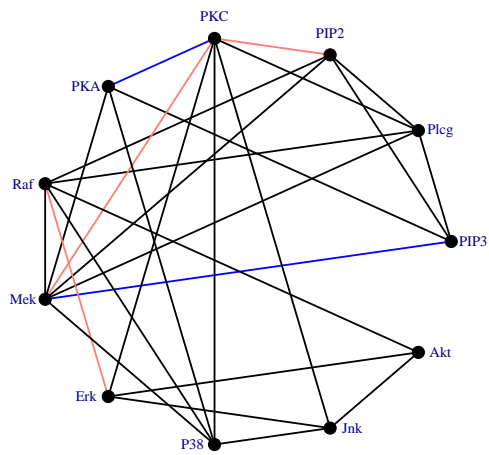


Figure 3: The best colored graph from flow cytometry data.

of random variables. Also, symmetry restrictions imposed on graphical Gaussian models reduce the number of parameters, which is useful when the number of variables exceeds the number of observations.

We develop a trans-dimensional double reversible jump algorithm, which provides an accurate estimate of Bayes factors. Combining linear regression with the double reversible jump algorithm, we develop an efficient model selection approach for colored graphical models. Our model selection approach avoids the calculation of normalizing constants of the colored G -Wishart distribution and saves computing time when p is large.

Appendix

This section contains the proofs of Theorems 5.1 and 6.1.

.1 Proof of Theorem 5.1

Given any model G with edge classes E_1, \dots, E_k and vertex classes V_1, \dots, V_t , the posterior probability of G given \mathbf{X} is:

$$p(G|\mathbf{X}) = \int_{\mathbf{K} \in P_G} p(G, \mathbf{K}|\mathbf{X}) d\mathbf{K} \propto \int_{\mathbf{K} \in P_G} p(\mathbf{X}|G, \mathbf{K}) p(\mathbf{K}|G) p(G) d\mathbf{K}.$$

We approximate $p(G|\mathbf{X})$ using the Laplace formula. For a given \mathbf{K} corresponding to the colored graph G , we rewrite \mathbf{K} as a $(k+t)$ -dimensional vector $\boldsymbol{\theta}$ with $\boldsymbol{\theta} = (\theta_{V_1}, \dots, \theta_{V_t}, \theta_{E_1}, \dots, \theta_{E_k})$. Let $q(\boldsymbol{\theta}, \mathbf{X}, G) = 1/n \times \log(p(\mathbf{X}|G, \boldsymbol{\theta})p(\boldsymbol{\theta}|G))$ and $\tilde{\boldsymbol{\theta}}$ be the mode of $q(\boldsymbol{\theta}, \mathbf{X}, G)$, where $p(G, \boldsymbol{\theta}|\mathbf{X})$

attains the maximum value. Then we have

$$\begin{aligned}
p(G|\mathbf{X}) &\propto p(G) \int_{\boldsymbol{\theta} \in P_G} p(\mathbf{X}|G, \boldsymbol{\theta}) p(\boldsymbol{\theta}|G) d\boldsymbol{\theta} \\
&= p(G) \int_{\boldsymbol{\theta} \in P_G} \exp\left\{n \frac{1}{n} \log(p(\mathbf{X}|G, \boldsymbol{\theta}) p(\boldsymbol{\theta}|G))\right\} d\boldsymbol{\theta} \\
&= p(G) \int_{\boldsymbol{\theta} \in P_G} \exp\left\{nq(\tilde{\boldsymbol{\theta}}, \mathbf{X}, G) - \frac{n}{2}(\boldsymbol{\theta} - \tilde{\boldsymbol{\theta}})^\top Q(\boldsymbol{\theta}^*, \mathbf{X})(\boldsymbol{\theta} - \tilde{\boldsymbol{\theta}})\right\} d\boldsymbol{\theta} \\
&= p(G) p(\mathbf{X}|G, \tilde{\boldsymbol{\theta}}) p(\tilde{\boldsymbol{\theta}}|G) (2\pi)^{\frac{d_G}{2}} n^{-\frac{d_G}{2}} |Q(\boldsymbol{\theta}^*, \mathbf{X})|^{-1/2} \\
&= \exp\left\{\log p(G) + nq(\tilde{\boldsymbol{\theta}}, \mathbf{X}, G) + \frac{1}{2}d_G \log 2\pi - \frac{1}{2}d_G \log n - \frac{1}{2} \log |Q(\boldsymbol{\theta}^*, \mathbf{X})|\right\},
\end{aligned}$$

where $Q(\boldsymbol{\theta}^*, \mathbf{X}) = -\partial^2 q(\boldsymbol{\theta}, \mathbf{X}, G) / \partial \boldsymbol{\theta} \partial \boldsymbol{\theta}^\top |_{\boldsymbol{\theta}^*}$, and $\boldsymbol{\theta}^*$ is within a small neighborhood of $\tilde{\boldsymbol{\theta}}$.

Following the definition in Højsgaard and Lauritzen (2008), we define the adjacency matrix \mathbf{T}^u for a edge or vertex color class u . For each vertex color class u , $u \in V_i, i = 1, \dots, t$, we define an $|V| \times |V|$ diagonal matrix \mathbf{T}^u with entries $T_{\alpha\alpha} = 1$ if $\alpha \in u$ and 0 otherwise. Similarly, for each color class u , $u \in E_j, j = 1, \dots, k$, we let \mathbf{T}^u be the $|V| \times |V|$ symmetric matrix with entries $T_{\alpha\beta}^u = 1$ if $(\alpha, \beta) \in u$ and 0 otherwise. We also have that

$$\begin{aligned}
q(\boldsymbol{\theta}, \mathbf{X}, G) &= \frac{1}{n} \log(p(\mathbf{X}|G, \mathbf{K}) p(\mathbf{K}|G)) \\
&= \frac{1}{n} \log \left\{ \frac{1}{I_G(\delta, \mathbf{D})} |\mathbf{K}|^{(n+\delta-2)/2} \exp\left\{-\frac{1}{2} \langle \mathbf{K}, \mathbf{S} + \mathbf{D} \rangle\right\} \mathbf{1}_{P_G}(\mathbf{K}) \right\} \\
&= \frac{1}{n} \left\{ -\log I_G(\delta, \mathbf{D}) + \frac{n+\delta-2}{2} \log |\mathbf{K}| - \frac{1}{2} \langle \mathbf{K}, \mathbf{S} + \mathbf{D} \rangle \right\} \mathbf{1}_{P_G}(\mathbf{K}).
\end{aligned}$$

By equation (6) in Højsgaard and Lauritzen (2008), we have that

$$\frac{\partial^2 q(\boldsymbol{\theta}, \mathbf{X}, G)}{\partial \theta^u \partial \theta^v} |_{\boldsymbol{\theta}^*} = -\frac{1}{n} \frac{n+\delta-2}{2} \text{tr}(\mathbf{T}^u \boldsymbol{\Sigma}^* \mathbf{T}^v \boldsymbol{\Sigma}^*)$$

for two color classes u and v , where $\text{tr}(\cdot)$ denotes the trace of a matrix, $\boldsymbol{\Sigma}^* = (\mathbf{K}^*)^{-1}$ which corresponds to $\boldsymbol{\theta}^*$. Thus, the term $\log |Q(\boldsymbol{\theta}^*, \mathbf{X})|$ is of order $O_p(1)$.

Let $\hat{\boldsymbol{\theta}}$ be the MLE. Now, we take the Taylor expansion of $\log p(\mathbf{X}|G, \tilde{\boldsymbol{\theta}})$ around $\hat{\boldsymbol{\theta}}$,

$$\log p(\mathbf{X}|G, \tilde{\boldsymbol{\theta}}) = \log p(\mathbf{X}|G, \hat{\boldsymbol{\theta}}) + \frac{1}{2}(\tilde{\boldsymbol{\theta}} - \hat{\boldsymbol{\theta}})^\top H(\boldsymbol{\theta}^{**}, \mathbf{X})(\tilde{\boldsymbol{\theta}} - \hat{\boldsymbol{\theta}}),$$

where $\boldsymbol{\theta}^{**}$ is vector in a small neighborhood of $\hat{\boldsymbol{\theta}}$ and $H(\boldsymbol{\theta}^{**}, \mathbf{X}) = -\partial^2 p(\mathbf{X}|G, \boldsymbol{\theta})/\partial\boldsymbol{\theta}\partial\boldsymbol{\theta}^\top|_{\boldsymbol{\theta}^{**}}$. Using similar arguments as for $Q(\boldsymbol{\theta}^*, \mathbf{X})$, we have that $H(\boldsymbol{\theta}^{**}, \mathbf{X})$ is of order $O_p(n)$. According to Theorem 4.3 in Ghosh et al. (2006), we have that $\sqrt{n}(\tilde{\boldsymbol{\theta}} - \hat{\boldsymbol{\theta}}) \rightarrow 0$ with a probability one. It implies $\tilde{\boldsymbol{\theta}} - \hat{\boldsymbol{\theta}} = O_p(1/\sqrt{n})$ and $(\tilde{\boldsymbol{\theta}} - \hat{\boldsymbol{\theta}})^\top H(\boldsymbol{\theta}^{**}, \mathbf{X})(\tilde{\boldsymbol{\theta}} - \hat{\boldsymbol{\theta}}) = O_p(1)$. Thus, $\log p(\mathbf{X}|G, \tilde{\boldsymbol{\theta}}) = \log p(\mathbf{X}|G, \hat{\boldsymbol{\theta}}) + O_p(1)$.

Let $\boldsymbol{\theta}_T$ be the parameter in the true model under which the data is generated. Let $\hat{\boldsymbol{\theta}}_T$, $\hat{\boldsymbol{\theta}}_s^+$ and $\hat{\boldsymbol{\theta}}_s^-$ be the MLEs corresponding to the true graph G_T , G_+ and G_- , respectively. Consider an under-fitting model with the underlying graph G_- , we define a pseudo true value $\boldsymbol{\theta}_-^*$ with

$$\boldsymbol{\theta}_-^* = \operatorname{argmin}_{\boldsymbol{\theta}_-} E_{\boldsymbol{\theta}_T} \left\{ \log \frac{p(\mathbf{X}|G_T, \boldsymbol{\theta}_T)}{p(\mathbf{X}|G_-, \boldsymbol{\theta}_-)} \right\}$$

under the misspecified model (White, 1982). By the weak Law of large numbers,

$$l(\hat{\boldsymbol{\theta}}_-)/n \xrightarrow{P} E_{\boldsymbol{\theta}_T} \{ \log p(\mathbf{X}|G_-, \boldsymbol{\theta}_-^*) \},$$

$$l(\hat{\boldsymbol{\theta}}_T)/n \xrightarrow{P} E_{\boldsymbol{\theta}_T} \{ \log p(\mathbf{X}|G_T, \boldsymbol{\theta}_T) \}.$$

This entails $l(\hat{\boldsymbol{\theta}}_-) - l(\hat{\boldsymbol{\theta}}_T) = E_{\boldsymbol{\theta}_T} \{ \log p(\mathbf{X}|G_-, \boldsymbol{\theta}_-^*) \} - E_{\boldsymbol{\theta}_T} \{ \log p(\mathbf{X}|G_T, \boldsymbol{\theta}_T) \} + o_p(n)$. Furthermore, $E_{\boldsymbol{\theta}_T} \{ \log p(\mathbf{X}|G_-, \boldsymbol{\theta}_-^*) \} < E_{\boldsymbol{\theta}_T} \{ \log p(\mathbf{X}|G_T, \boldsymbol{\theta}_T) \}$ due to the Kullback-Leibler inequality. Combining the results above, we have

$$\begin{aligned} & \log \frac{p(G_T | \mathbf{X})}{p(G_- | \mathbf{X})} \\ &= \log \int_{\boldsymbol{\theta} \in P_{G_T}} p(\mathbf{X}|G_T, \boldsymbol{\theta}) p(\boldsymbol{\theta}|G_T) d\boldsymbol{\theta} - \log \int_{\boldsymbol{\theta} \in P_{G_-}} p(\mathbf{X}|G_-, \boldsymbol{\theta}) p(\boldsymbol{\theta}|G_-) d\boldsymbol{\theta} \\ &= \log p(\mathbf{X}|G_T, \tilde{\boldsymbol{\theta}}_T) - \log p(\mathbf{X}|G_-, \tilde{\boldsymbol{\theta}}_-) + \log p(\tilde{\boldsymbol{\theta}}_T | G_T) - \log p(\tilde{\boldsymbol{\theta}}_- | G_-) \\ &\quad - \frac{1}{2} d_{G_T} \log n + \frac{1}{2} d_{G_-} \log n + O_p(1) \\ &= [l(\hat{\boldsymbol{\theta}}_T) - l(\hat{\boldsymbol{\theta}}_-)] + \frac{1}{2} (d_{G_-} - d_{G_T}) \log n + O_p(1) \\ &= n(E_{\boldsymbol{\theta}_T} \{ \log p(\mathbf{X}|G_T, \boldsymbol{\theta}_T) \} - E_{\boldsymbol{\theta}_T} \{ \log p(\mathbf{X}|G_-, \boldsymbol{\theta}_-^*) \}) + \frac{1}{2} (d_{G_-} - d_{G_T}) \log n + o_p(n). \end{aligned}$$

The second last equality holds because $p(\boldsymbol{\theta}|G)$ is the colored G -wishart prior defined in (1), and $\log p(\tilde{\boldsymbol{\theta}}|G)$ is a $O_p(1)$ term with respect to the sample size n . In the last equality, the first term is the dominating term. Due to the KL inequality above and the fact that $d_{G_-} < d_{G_T}$, the last line is asymptotically positive. Thus, we have $p(G_T|\mathbf{X}) > p(G_-|\mathbf{X})$ with probability tending to one when n goes to infinity.

Consider an over-fitting model with the underlying graph G_+ , we have that

$$\begin{aligned} & \log \int_{\boldsymbol{\theta} \in P_{G_T}} p(\mathbf{X}|G_T, \boldsymbol{\theta}) p(\boldsymbol{\theta}|G_T) d\boldsymbol{\theta} - \log \int_{\boldsymbol{\theta} \in P_{G_+}} p(\mathbf{X}|G_+, \boldsymbol{\theta}) p(\boldsymbol{\theta}|G_+) d\boldsymbol{\theta} \\ &= \log p(\mathbf{X}|G_T, \tilde{\boldsymbol{\theta}}_T) - \log p(\mathbf{X}|G_+, \tilde{\boldsymbol{\theta}}_+) - \frac{1}{2} d_{G_T} \log n + \frac{1}{2} d_{G_-} \log n + O_p(1) \\ &= [l(\hat{\boldsymbol{\theta}}_T) - l(\hat{\boldsymbol{\theta}}_+)] + \frac{1}{2} (d_{G_+} - d_{G_T}) \log n + O_p(1). \end{aligned}$$

According to the standard asymptotic theory for the loglikelihood ratio statistics, we have that $-2\{l(\hat{\boldsymbol{\theta}}_T) - l(\hat{\boldsymbol{\theta}}_+)\} \sim \chi_{d_{G_T} - d_{G_+}}^2 = O_p(1)$. Therefore, the dominating term is the second term. As $d_{G_+} > d_{G_T}$, then $p(G_T|\mathbf{X}) > p(G_+|\mathbf{X})$ with probability tending to one when n goes to infinity.

.2 Proof of Theorem 6.1

We write the Cholesky decomposition of \mathbf{K} under the form $\mathbf{K} = \mathbf{A}\mathbf{A}^\top$ with

$$A_{ij} = \begin{cases} \sqrt{a_{ii}} & \text{if } i = j, \\ -a_{ij} & \text{if } i < j. \end{cases}$$

Thus, the entries of $\mathbf{A}\mathbf{A}^\top$ are given by

$$(AA^\top)_{ij} = \begin{cases} a_{ii} + \sum_{l>i} a_{il}^2 & \text{if } i = j, \\ -a_{ij}\sqrt{a_{jj}} + \sum_{l>\max\{i,j\}} a_{il}a_{jl} & \text{if } i < j. \end{cases}$$

For the colored graph shown in Figure 1 (e), we denote the corresponding precision matrix by

$$\mathbf{K} = \begin{pmatrix} K_{11} & K_{12} & 0 \\ K_{12} & K_{22} & 0 \\ 0 & 0 & K_{22} \end{pmatrix}.$$

Since $K_{13} = 0$ and $a_{33} > 0$, we have $a_{13} = 0$. In addition, the conditions $K_{23} = 0$ and $a_{33} > 0$ imply $a_{23} = 0$. It follows that

$$\mathbf{K} = \begin{pmatrix} a_{11} + a_{12}^2 & -a_{12}\sqrt{a_{22}} & 0 \\ -a_{12}\sqrt{a_{22}} & a_{22} & 0 \\ 0 & 0 & a_{33} \end{pmatrix}.$$

It can be seen from $K_{22} = K_{33}$ that $a_{22} = a_{33}$. Now we can write \mathbf{K} as

$$\mathbf{K} = \begin{pmatrix} a_{11} + a_{12}^2 & -a_{12}\sqrt{a_{22}} & 0 \\ -a_{12}\sqrt{a_{22}} & a_{22} & 0 \\ 0 & 0 & a_{33} \end{pmatrix}$$

and $|\mathbf{K}| = a_{11}a_{22}^2$. On the other hand, the Jacobian of the transformation from \mathbf{K} to \mathbf{A} is

$$\mathbf{J} = \begin{matrix} & k_{11} & k_{12} & k_{22} \\ \begin{matrix} a_{11} \\ a_{12} \\ a_{22} \end{matrix} & \begin{pmatrix} 1 & 0 & 0 \\ * & -\sqrt{a_{22}} & 0 \\ * & * & 1 \end{pmatrix} \end{matrix}.$$

We obtain $|\mathbf{J}| = a_{22}^{1/2}$ and

$$\langle \mathbf{K}, \mathbf{D} \rangle = d_{11}(a_{11} + a_{12}^2) + d_{22}a_{22} + d_{33}a_{22} + 2d_{12}(-a_{12}\sqrt{a_{22}}).$$

Therefore the normalizing constant $I_G(\delta, \mathbf{D})$ can be written as

$$\int_{\mathbf{A}} a_{11}^{\frac{\delta-2}{2}} a_{22}^{\delta-3/2} \exp \left\{ -\frac{1}{2}d_{11}a_{11} - \frac{1}{2}d_{11}a_{12}^2 - \frac{1}{2}(d_{22} + d_{33})a_{22} + d_{12}a_{12}\sqrt{a_{22}} \right\} d\mathbf{A},$$

where $a_{ii} > 0$, $a_{ij} \in R$, $i < j$, and $d\mathbf{A}$ denotes the product of all differentials. In the above integral, we have that the integral with respect to a_{11} is a gamma integral with

$$\int_0^\infty a_{11}^{\frac{\delta-2}{2}} \exp(-\frac{1}{2}d_{11}a_{11})da_{11} = 2^{\frac{\delta}{2}}\Gamma(\frac{\delta}{2})d_{11}^{-\frac{\delta}{2}}.$$

The integral with respect to a_{12} is a Gaussian integral with

$$\int_{-\infty}^\infty \exp(-\frac{1}{2}d_{11}a_{12}^2 + d_{12}\sqrt{a_{22}}a_{12})da_{12} = \frac{\sqrt{2\pi}}{\sqrt{d_{11}}} \exp(\frac{d_{12}^2 a_{22}}{2d_{11}}).$$

After some simplifications, we have

$$\begin{aligned} I_G(\delta, \mathbf{D}) &= 2^{\frac{\delta}{2}}\Gamma(\frac{\delta}{2})d_{11}^{-\frac{\delta}{2}} \frac{\sqrt{2\pi}}{\sqrt{d_{11}}} \int_0^\infty a_{22}^{\delta-\frac{3}{2}} \exp\left\{-\frac{1}{2}(d_{22} + d_{33})a_{22} + \frac{d_{12}^2}{2d_{11}}a_{22}\right\} da_{22} \\ &= \frac{2^{\frac{\delta+1}{2}}\Gamma(\frac{\delta}{2})\sqrt{\pi}d_{11}^{-\frac{\delta+1}{2}}\Gamma(\delta - \frac{1}{2})}{[\frac{1}{2}(d_{22} + d_{33}) - \frac{d_{12}^2}{2d_{11}}]^{\delta-\frac{1}{2}}}. \end{aligned}$$

Acknowledgements

The authors would like to acknowledge Sagnik Datta for his assistance in programming.

References

- Atay-Kayis, A. and Massam, H. (2005). A Monte Carlo method for computing the marginal likelihood in nondecomposable Gaussian graphical models. *Biometrika*, 92(2):317–335.
- Dobra, A., Hans, C., Jones, B., Nevins, J. R., Yao, G., and West, M. (2004). Sparse graphical models for exploring gene expression data. *Journal of Multivariate Analysis*, 90(1):196–212.
- Dobra, A., Lenkoski, A., and Rodriguez, A. (2011). Bayesian inference for general Gaussian graphical models with application to multivariate lattice data. *Journal of the American Statistical Association*, 106(496):1418–1433.

- Gehrmann, H. (2011). Lattices of graphical Gaussian models with symmetries. *Symmetry*, 3(3):653–679.
- Ghosh, J. K., Delampady, M., and Samanta, T. (2006). *An Introduction to Bayesian Analysis: Theory and Methods*. New York: Springer.
- Green, P. J. (1995). Reversible jump Markov chain Monte Carlo computation and Bayesian model determination. *Biometrika*, 82(4):711–732.
- Hastie, T., Tibshirani, R., and Friedman, J. (2009). *The Elements of Statistical Learning: Data Mining, Inference, and Prediction*. New York: Springer-Verlag.
- Højsgaard, S. and Lauritzen, S. L. (2007). Inference in graphical Gaussian models with edge and vertex symmetries with the gRc package for R. *Journal of Statistical Software*, 23(6):1–26.
- Højsgaard, S. and Lauritzen, S. L. (2008). Graphical Gaussian models with edge and vertex symmetries. *Journal of the Royal Statistical Society: Series B (Statistical Methodology)*, 70(5):1005–1027.
- Jung, S.-Y., Park, Y. C., Choi, K.-S., and Kim, Y. (1996). Markov random field based English part-of-speech tagging system. In *Proceedings of the 16th Conference on Computational Linguistics*, pages 236–242. Association for Computational Linguistics, Stroudsburg, PA.
- Lenkoski, A. (2013). A direct sampler for G-wishart variates. *Stat*, 2(1):119–128.
- Leppä-aho, J., Pensar, J., Roos, T., and Corander, J. (2017). Learning Gaussian graphical models with fractional marginal pseudo-likelihood. *International Journal of Approximate Reasoning*, 83:21–42.
- Li, S. Z. (2001). *Markov Random Field Modeling in Image Analysis*. New York: Springer.

- Liang, F. (2010). A double Metropolis–Hastings sampler for spatial models with intractable normalizing constants. *Journal of Statistical Computation and Simulation*, 80(9):1007–1022.
- Massam, H., Li, Q., and Gao, X. (2018). Bayesian precision and covariance matrix estimation for graphical Gaussian models with edge and vertex symmetries. *Biometrika*, 105(2):371–388.
- Meinshausen, N. and Bühlmann, P. (2006). High-dimensional graphs and variable selection with the lasso. *The Annals of Statistics*, 34(3):1436–1462.
- Murray, I., Ghahramani, Z., and MacKay, D. J. C. (2006). MCMC for doubly-intractable distributions. In *Proceedings of the 22nd Annual Conference on Uncertainty in Artificial Intelligence*, pages 359–366. Cambridge, MA: AUAI Press.
- Sachs, K., Perez, O., Pe’er, D., Lauffenburger, D. A., and Nolan, G. P. (2005). Causal protein-signaling networks derived from multiparameter single-cell data. *Science*, 308(5721):523–529.
- Shen, X., Huang, H.-C., and Pan, W. (2012). Simultaneous supervised clustering and feature selection over a graph. *Biometrika*, 99(4):899–914.
- Wang, H. and Li, S. Z. (2012). Efficient Gaussian graphical model determination under G-wishart prior distributions. *Electronic Journal of Statistics*, 6:168–198.
- White, H. (1982). Maximum likelihood estimation of misspecified models. *Econometrica*, 50:1–25.